

EXPERIMENTAL CHARACTERIZATION OF CARBON-EPOXY COMPOSITE MATERIAL FLEXURAL RIGIDITY *

Gabriel P. de Araujo¹
Gigliola Salerno²

Abstract

The carbon-epoxy composite has high specific resistance and strength, which means specific applications. However, its behavior under compressive stress could be decreased by delamination, needing more detailed studies. The main purpose of the present work is to verify the mechanical properties in bending process considering two different fiber orientations. The composite materials were made by woven fibers and epoxy resin. Primarily, the carbon fiber fabrics suffered a superficial physical treatment called silanization, in order to developing a better chemical adhesion between fibers and resin. After the superficial treatment, the layers were embedded with epoxy resin. The composite resin's cure was made in a Fanem heater, model 320, during 1 hour at 120°C at 1.5 bar; subsequently the specimens were cut by water jet. Specimens oriented in 0°/90° and 0°/90°/45 were manufactured and taken to bending tests, accordingly to the ASTM E855 and D790 standards, in an universal testing machine MTS – Material Test System, full capacity of 250 kN. It was concluded that all specimens failed by tension. Specimens with internal void volumes results in lower flexural modulus and those with presence of fracture mechanisms, like delamination, showed lower strength values. Scanning Electronic Microscopy demonstrated the damages involved during bending process.

Keywords: Laminated, Carbon-epoxy, Bending, Orientation.

¹ Mechanical engineering, Student, Engenharia Mecânica, Centro Universitário da FEI, São Paulo, São Paulo, Brazil.

² PhD, Professor, Engenharia de Materiais, Centro Universitário da FEI, São Paulo, São Paulo, Brazil.

1 INTRODUCTION

Composite materials are applied in many applications due high values of specific stiffness and resistance. In recent years industry substituted steel and aluminum for composites, in addition to their low density. Comparing steel and composites, specific resistance could be five times higher than the first one [1]. However, manufacturing costs are much higher for composites materials, which can provide some difficulties in expand their applications in ordinary industry [2].

In a way to improve mechanical behavior, different fiber orientation (unidirectional or woven) [3], thickness, length, number of layers, should be studied. The main purpose of this work was manufacturing carbon epoxy composite material, in the woven fiber different orientation like $0^\circ/90^\circ$ and $0^\circ/90^\circ/\pm 45^\circ$ and characterizes the bending response in three point bending tests in an universal testing MTS - Material Test System (250 kN full capacity) up to the failure according to ASTM E855 e D790 standards [4, 5]. Elasticity modulus E (equation 1), strength σ (equation 2) and strain ϵ (equation 3) were obtained and compared, in which F indicates force applied in the mid spam L . Dimensions b and h indicate width and thickness of the transversal area, respectively; δ indicates deflexion.

$$E = \frac{FL^3}{4\delta bh^3} \quad (1)$$

$$\sigma = \frac{3FL}{2bh^2} \quad (2)$$

$$\epsilon = \frac{6h\delta}{L^2} \quad (3)$$

The matrix, primarily, responds at the loading, protects e transfers the loading to the fibers, in that way adhesion fiber/resin can provide better resistance. A superficial treatment, called silanization, try to improve this adhesion [6]. Silane is a polymer in which some particles interacts with the resin and some interacts the fiber, promoting better adhesion [6, 7, 8].

According to Davies [9], unidirectional carbon epoxy composites, 135 x 12.7 x 1 mm dimensions have elasticity modulus about 50 GPa. It will be expected that in this work, the elasticity modulus be at the same magnitude, however, it will be lower because of woven bidirectional fibers [10].

2 MATERIAL AND METHODS

Specimen dimensions and fiber orientation are presented in table 1. Specimens $0^\circ/90^\circ/\pm 45^\circ$ were manufacturing $0^\circ/90^\circ$ and $45^\circ/-45^\circ$ symmetric and balanced layers. During the initial production (CP-1 a CP-6 specimens), some macroscopic voids were observed creating an initial delamination. Bending mechanical behavior were analyzed in order to verify its influence. After the solution was found, the next specimens (CP-7 a CP-20) did not present that defect and fiber orientation influence could be analyzed.

Table 1. Dimensions and fibers orientation for all specimens

Specimen	Dimensions [mm]	Orientation
1 - 6	210 x 60 x 12	$0^\circ/90^\circ$
7 - 13	240 x 50 x 10	$0^\circ/90^\circ$
14 - 20	240 x 50 x 10	$0^\circ/90^\circ/\pm 45^\circ$

Silanization was the first procedure; the woven fibers were submerged in a silane, water and acetone solution for one hour. In the subsequent step, were dried by air for eight hours. Acetone purpose was eliminated air bubbles created during chemical reaction between water and silane, in that way did not allow their adhesion to fibers in order to avoid defects like microvoids. Subsequently the silanization, resin epoxy (AR-260 and AH-260 catalyzer) was impregnated in which layer, and disposed one by one, according the fiber orientation desired ($0^\circ/90^\circ$ or $\pm 45^\circ$). After composite lamination, it were cured in a furnace FANEM, model 320, at 120°C for one hour at 1.5 bar. Cooling was realized at $20^\circ\text{C}/\text{hour}$. The composite was cut by water jet in order to provide better dimensions tolerances and avoid fibers fractured on the edges. According to ASTM E855 e D790 standards [4, 5], specimens CP7- CP20 were tested on bending in an universal testing machine MTS – Material Test System, full capacity of 250 kN at 6,5 mm/min velocity. Specimens CP1 –CP6 were tested on bending at 5 mm/min velocity. In order to observe and identify damage mechanisms, Scanning Electron Microscopy was realized.

In order to obtain density and mass fiber and mass resin, a small composite piece was cut and heating on vacuum furnace Jung® at 500°C for one hour. At this temperature, resin evaporated and the remained fiber mass could be measured. Describe succinctly the equipment and procedures used, as the literature and the statistical methods and the corresponding literature, as the case demands.

3 RESULTS AND DISCUSSION

Density and mass fraction of fiber and resin were identify for each specimen groups and are summarized in table 2. These values were similar to Davies and Deng works [9, 10], which can provide some discussions about bending. During water jet cut, the tolerance dimensions were attained (Fig.1) without fracture of fibers or defects on the edges. However, during lamination some macro voids were found in CP1, CP2 and CP3 specimen thickness, concluding that manual pressure was not efficient to accommodate layer over layer. Voids can be found in composites produced by manual lamination process, especially when the plate is thick, about 10 mm or more.

Table 2. Density, percent of fibers and resin masses

Specimen	Density [g/cm ³]	Fiber mass %	Resin mass %
1 - 6	1.61	52.2	47.8
7 - 13	1.23	59.5	40.5
14 - 20	1.27	58.3	41.7

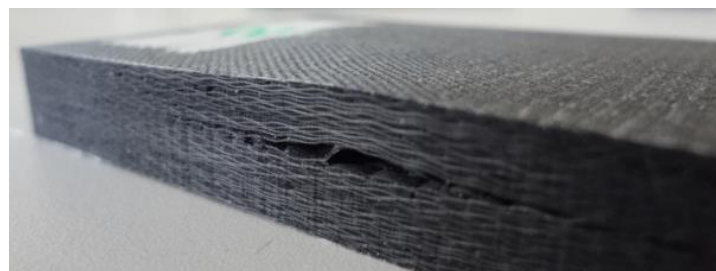


Figure 1. Void found in specimen CP2.

Three-point bending tests were performed in all specimens (Fig. 2). The bending behavior of CP1 – CP6 specimens are shown in a stress-strain curve (Fig. 3).

Mechanical bending properties as modulus of elasticity (E), flexural strength (σ_{\max}), rupture stress (σ_R) and rupture strain (ϵ_R) (table 3) were obtained according to equations 1 to 3. Can be observed in these results that specimens containing voids has smaller maximum stress values because these voids acted like delaminations.



Figure 2. Specimen during three-point bending test, load at the midpoint and supports.

Table 3. Mechanical flexural properties for specimens 1 - 6.

Engineering constant		
E	33 ± 1	[GPa]
σ_{\max}	302 ± 25	[MPa]
σ_R	278 ± 47	[MPa]
ϵ_R	1.29 ± 0.09	[%]

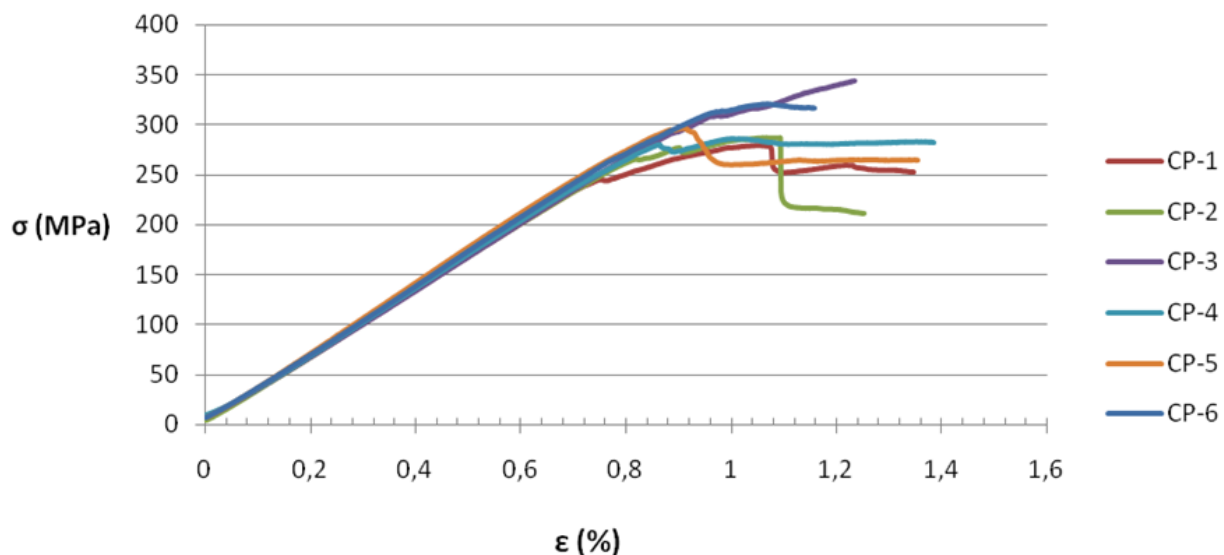


Figure 3. Stress-strain curve for 1 - 6 specimens.

Another group of specimens were manufacturing without voids or defects, pressing the laminate using a metallic roll. The bending behavior of CP7 – CP13 specimens are shown in a stress-strain curve (Fig. 4). Mechanical bending properties as modulus of elasticity (E), flexural strength (σ_{\max}), rupture stress (σ_R) and rupture strain (ϵ_R) (table 4) were obtained according to equations 1 to 3. In figure 5 is shown specimen CP8 after bending which presented a delamination in the compression

region and fracture in the tensile region. All the specimens presented tensile failure in the outer fibers of the beam along their lower face.

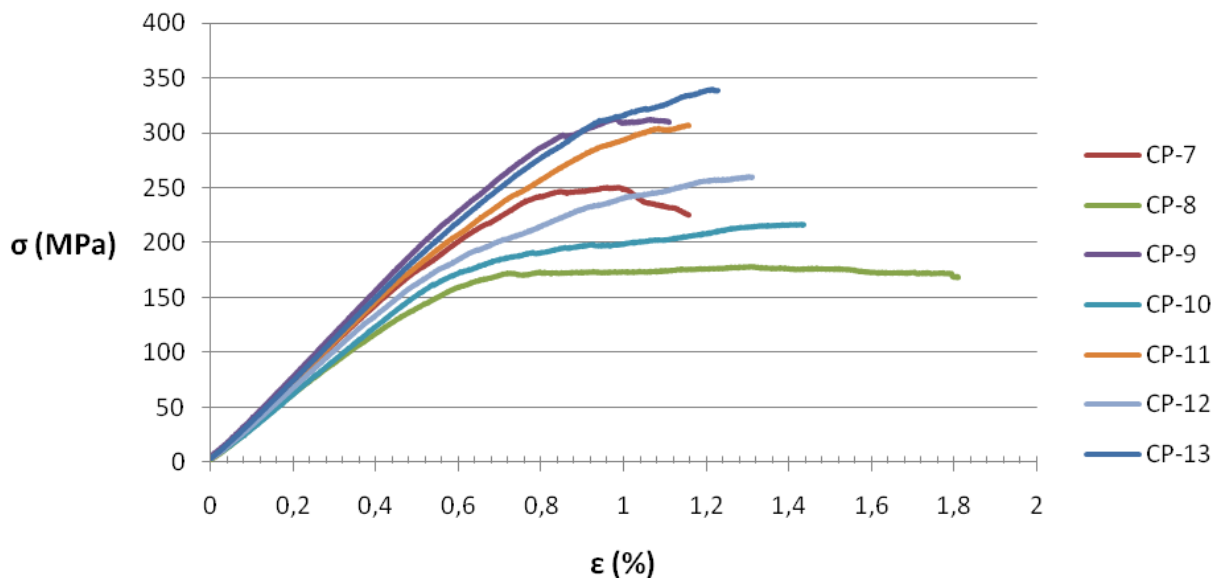


Figure 4. Stress-strain curve for 7 - 13 specimens.

Table 4. Mechanical flexural properties for specimens 7 - 13.

Engineering constant		
E	34 ± 4	[GPa]
σ_{\max}	266 ± 57	[MPa]
σ_R	260 ± 61	[MPa]
ϵ_R	1.32 ± 0.24	[%]

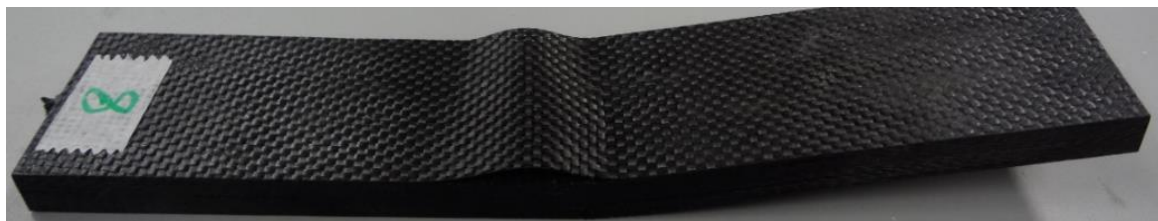


Figure 5. Specimen CP8 after bending test.

Modulus of elasticity were according to literature, in the same magnitude [9, 10]. Specimens that presented lower flexural resistance presented delamination inner fibers of the beam along their higher face (Fig. 6). However, the principal damage mechanism was tensile fiber fracture on outer fibers of the beam along their lower face (Fig. 6). Delaminations outer or inner fibers of the beam influenced directly flexural properties. Specimens CP-1 to CP-6 and CP-7 to CP-13, was observed that tensile fiber fracture on outer fibers of the beam along their lower face was the most important damage, i.e., specimens lost the flexural resistance when fibers failure.

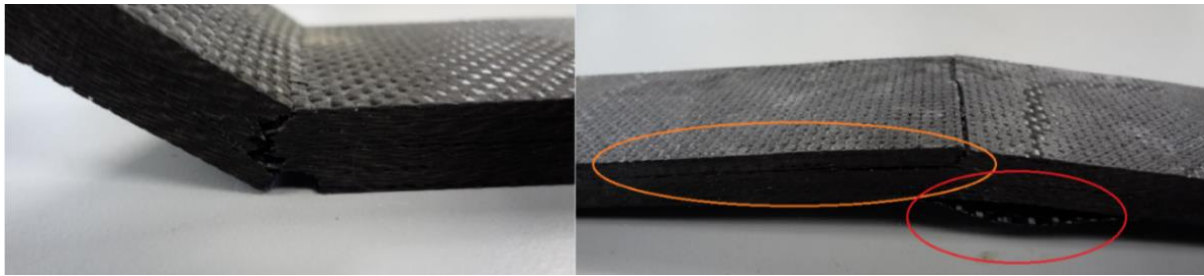


Figure 6. Comparison between CP-13 (on left) and CP-8 (on right) fractures. Delamination outer fibers of the beam along its lower face indicated by orange ellipse. Delamination inner fibers of the beam along its higher face indicated by red ellipse. Fiber fracture outer fibers of the beam along its lower face for CP13.

The bending behavior of CP14 – CP20 specimens are shown in a stress-strain curve (Fig. 7). These specimens presented $\pm 45^\circ$ layers. Mechanical bending properties as modulus of elasticity (E), flexural strength (σ_{\max}), rupture stress (σ_R) and rupture strain (ϵ_R) (table 5) were obtained according to equations 1 to 3.

Table 5. Mechanical flexural properties for specimens 14 - 20.

Engineering constant		
E	24 ± 4	[GPa]
σ_{\max}	275 ± 57	[MPa]
σ_R	264 ± 61	[MPa]
ϵ_R	1.46 ± 0.18	[%]

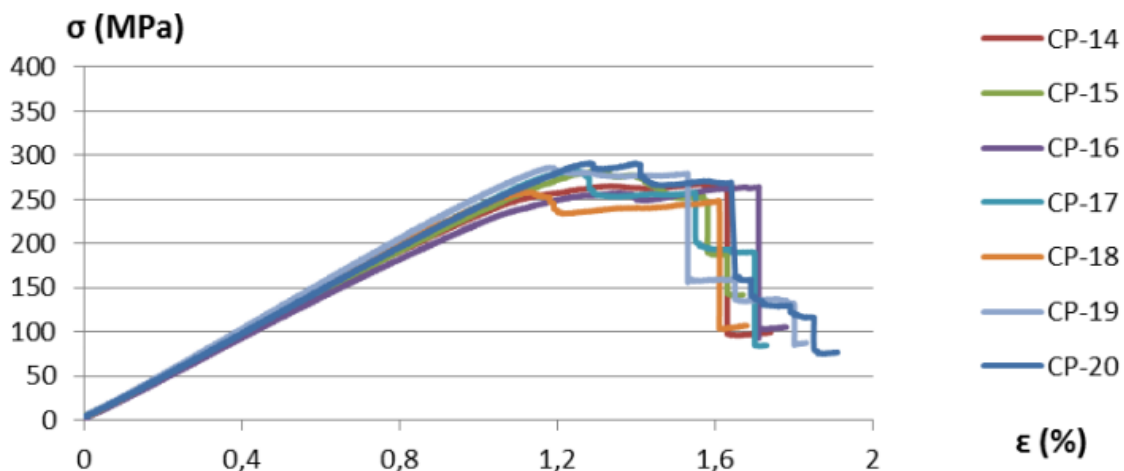


Figure 7. Stress-strain curve for 14 - 20 specimens.

Despite the fact that the results presented the same magnitude as the composite laminates in $0^\circ/90^\circ$ fibers orientation, is possible analyze that modulus of elasticity were significantly lower. This fact could be explained by fiber direction $\pm 45^\circ$, which provokes anisotropy, changing the mechanical behavior related to the applied load. Modulus of elasticity for $0^\circ/90^\circ$ fibers orientation was obtained 34 GPa (table 4), for $0^\circ/90^\circ/\pm 45^\circ$ fibers orientation was 24 GPa (table 5), which represents a reduction of 29%.

In another way, flexural strength presented higher values for $0^\circ/90^\circ/\pm 45^\circ$ fibers orientation, approximately 3.2% and 9.6 % for rupture strain. This fact is based on the delamination process; it did not occur in $0^\circ/90^\circ/\pm 45^\circ$ fibers orientation. The only damage mechanism was tensile fiber fracture on outer fibers of the beam along its

lower face (Fig. 8). When delamination occur, resistance and stiffness of the material reduce. In addition to this, the rupture strain was superior in $0^\circ/90^\circ/\pm 45^\circ$ fibers orientation specimens. In figure 7 can be observed that damage was continuous, specimens did not fracture rapidly, in that way, the most of the specimens after some abrupt reducing in the stress, some fibers could continue to resist showing that crack propagation was stable in some levels of load, which guarantee toughness.

In specimens CP-14 to CP-20 was observed that fiber fracture on outer fibers of the beam along their lower face was the most important damage, i.e., specimens lost the flexural strength when fibers failure. However, differently to the other specimens, no delamination was presented and some layer remains without any fiber fracture. In figure 8 it is possible to observe the fracture.



Figure 8. Fracture in specimen CP20. It is possible observe only fiber fracture on outer fibers of the beam along its lower face.

3.1 Scanning electron microscopy

CP1 image of the thickness along the width (figure 9) shows evidences of the woven layer $0^\circ/90^\circ$ (red ellipse) and fiber fracture on outer fibers 0° of the beam along their lower face (orange ellipse). In image of the thickness along the length, red narrows indicate delaminations that probably initiated in microvoids and green narrows indicate beginning and end of fracture of fibers.

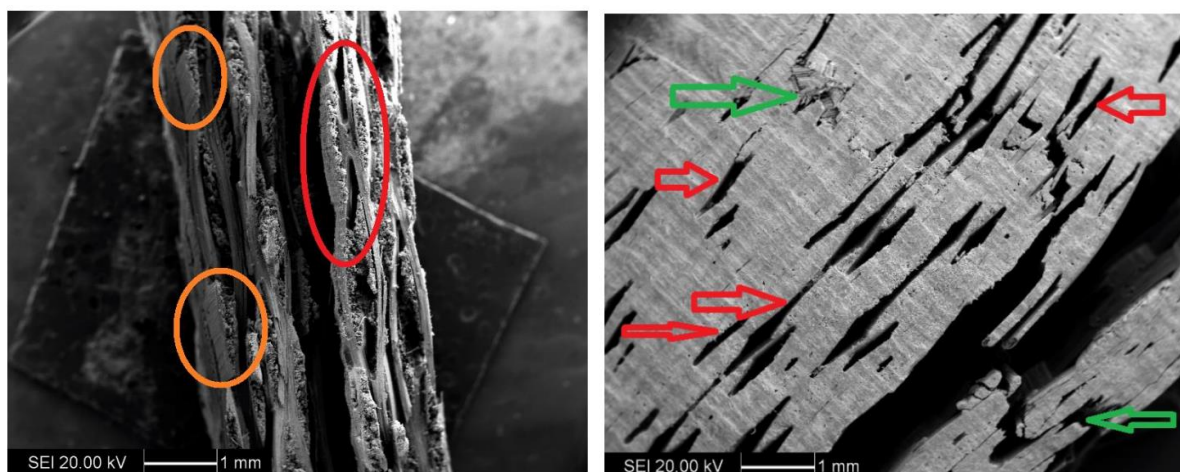


Figure 9. Scanning electron microscopy images of CP 1, fiber fracture and delaminations.

CP8 images of the thickness along the width (figure 10) shows pull out fibers (yellow narrows) and resin crack propagation (green ellipse). In image of the thickness along

the length, green narrows indicates crack initiated in microvoid, propagated transversally in the resin and created a delamination, separating the layers.

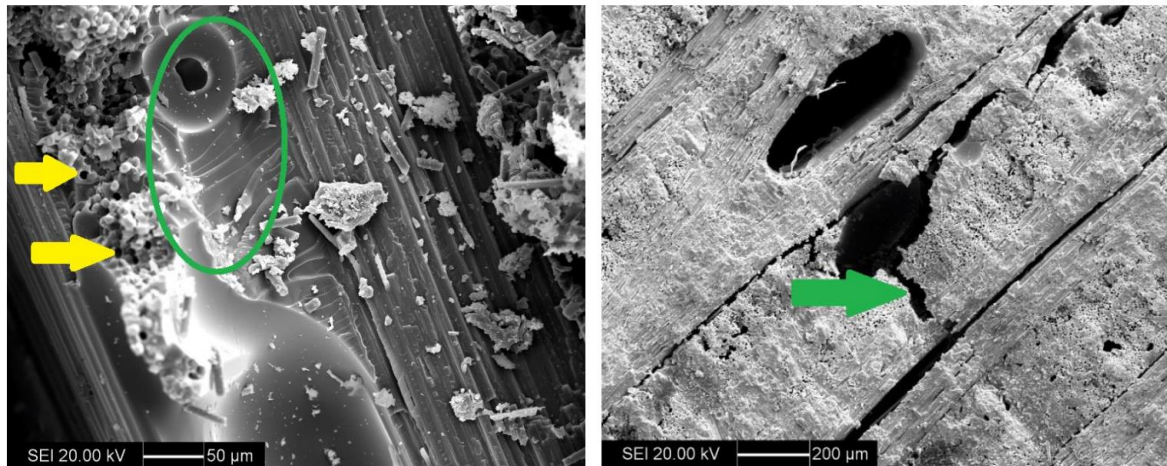


Figure 10. Scanning electron microscopy images of CP8, pullout fibers and crack propagation in the resin.

CP17 image of the thickness along the length of $0^\circ/90^\circ/\pm 45^\circ$ fibers orientation (figure 11) shows the failure sequence: resin crack propagated transversally (yellow narrow) that passed through a void (red ellipse) that finally provoked a delamination (green narrow). All the red ellipses show voids. In image of the thickness along the width, can be observed fiber fracture on outer fibers of the beam along its lower face, the $0^\circ/90^\circ$ layers fracture near the surface, however $45^\circ/-45^\circ$ layers did not, emphasizing the different behavior of $45^\circ/-45^\circ$ layers (yellow narrows).

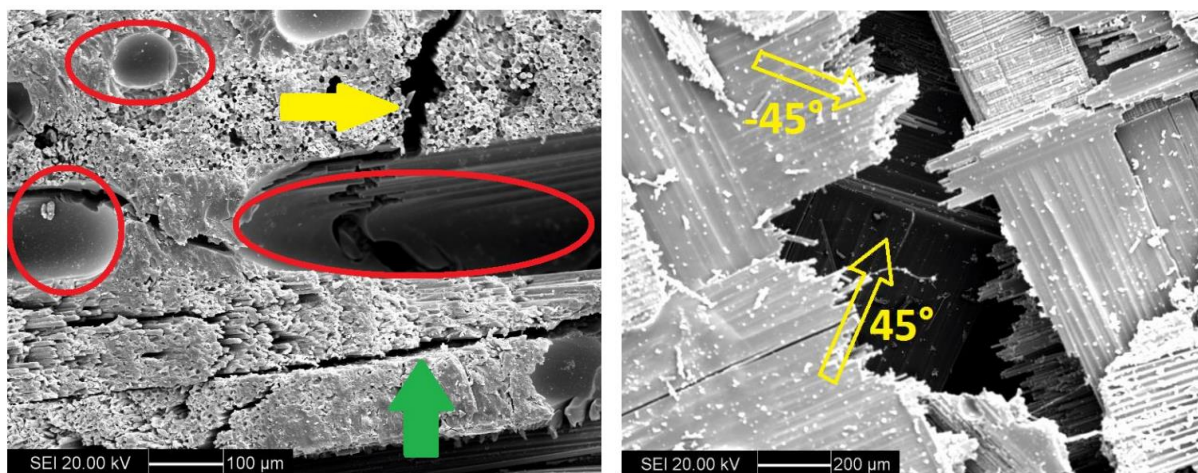


Figure 11. Scanning electron microscopy images of CP17, voids, delamination e fibers fracture.

4 CONCLUSION

During water jet cut, the tolerance dimensions were attained without fracture of fibers or defects on the edges considering the plate were thick. Manual manufacturing laminates without voids or defects were obtained pressing the laminate using a metallic roll.

Specimens CP7-CP20 presented similar density and fiber mass, in that way only fiber orientation was the variable.

During the tests, specimens in that occurred delamination process during bending showed lower values of flexural strength. Independently of the fact that delamination occurred; all the specimens had tensile fiber fracture on outer fibers of the beam along their lower face.

In terms of stiffness, $0^\circ/90^\circ$ composite laminate had mean values approximately 42.5% higher than $0^\circ/90^\circ/\pm 45^\circ$ composite laminate. However, in terms of resistance, $0^\circ/90^\circ/\pm 45^\circ$ composite laminate had mean values approximately 3.2% higher than $0^\circ/90^\circ$ composite laminate. This fact is based on the delamination process; it did not occur in $0^\circ/90^\circ/\pm 45^\circ$ fibers orientation. The only damage mechanism was fiber fracture on outer fibers of the beam along its lower face. In addition, strain values were higher approximately 9.6 % for rupture strain, which indicated higher toughness.

Comparing both of laminates, could be concluded that in terms of flexural strength the difference between them were not so significantly, however in terms of delamination process $0^\circ/90^\circ/\pm 45^\circ$ had better response and in terms of stiffness $0^\circ/90^\circ$ could be a better choice. .

REFERENCES

- 1 Chawla KK. Composite Materials – Science and Engineering, 2^a. Ed. 1998.
- 2 Bäker M, Rösler J, Harders H. Mechanical behaviour of engineering materials. Springer Science, Berlin, 2007.
- 3 Boisse, P. Simulations of Woven Composite Reinforcement Forming. Woven Fabric Engineering, 387-414. Polona Dobnik Dubrovski, ISBN 978-953-307-194-7, 2010.
- 4 American Society for Testing and Materials (ASTM). Standard Test Methods for Bend Testing of Metallic Flat Materials for Spring Applications Involving Static Loading. Standard E, 855-08 edition, 2008.
- 5 American Society for Testing and Materials (ASTM). Standard test method Flexural properties of unreinforced and reinforces plastics and electrical insulating materials. Standard D, 790-07 edition, 2007.
- 6 Burakowski L, Rezende MC. Modificação da Rugosidade de Fibras de Carbono por Método Químico para Aplicação em Compósitos Poliméricos. Polímeros: Ciência e Tecnologia, vol. 11, n^o 2, p. 51-57, 2001.
- 7 Neto FL, Pardini LC. Compósitos estruturais: ciência e tecnologia. 1^a ed. São Paulo. Blücher. 2006.
- 8 Rezende, MC, Costa ML, Botelho EC. Compósitos estruturais: tecnologia e prática. 1^a ed. São Paulo: Artliber. 2011.
- 9 Davies SIJ. The effect of processing parameters on the flexural properties of unidirectional carbon-fiber reinforced polymer (CFRP) composites. Materials Science and Engineering A. 498:65-68. 2008.
- 10 Deng S, Ye L, Mai YW. Influence of fiber cross-section aspect ratio on mechanical properties of glass fiber epoxy composites. Composites Science and Technology. 59: 1331-1339. 1998.